

On the Analysis of the Dynamics and Synchronization of chaotic modulation and demodulation in UWB Communication and Positioning Systems

J. C. Chedjou^{1*}, J. P. Dada², I. Moussa², C. Takenga³, R. Anne³, and K. Kyamakya³

¹International Centre for Theoretical Physics (ICTP), Strada Costiera 11, 34014 Trieste, Italy and Department of Physics, Faculty of Science, University of Dschang, P.O. Box 67, Dschang, Cameroon

²Department of Physics, Faculty of Science, University of Yaoundé-I, P.O. Box 812, Yaoundé, Cameroon

³ Institut für Allgemeine Nachrichtentechnik, Universität Hannover, Appelstraße 9A, 30167, Hannover, Germany

* Corresponding author: Department of Physics, Faculty of Science, University of Dschang, P.O. Box 67, Dschang, Cameroon, email: chedjou@ant.uni-hannover.de

Abstract— This paper studies synchronization transitions in a system of coupled non-identical self-sustained chaotic oscillators of the Rössler type. The interest devoted to the Rössler oscillators is motivated by their capability to behave chaotically at very high frequencies. Both phase synchronization and lag synchronization are analyzed in terms of a coupling parameter. It is shown that the both types of synchronization can be achieved when monitoring a coupling parameter. The advantage of using one parameter to insure both types of synchronization is found in practical realizations. Indeed one should monitor only one resistor to predict the boundaries of the control resistor for the occurrence of each type of synchronization. Another advantage of monitoring only one resistor is found in the accuracy of results. An experimental study of the synchronization is carried out. Experimental waveforms in the drive and response systems are obtained. The waveforms are compared to confirm the achievement of synchronization experimentally. One of the advantages of using analog simulation in this work is the possibility to analyze the behaviour of the coupled system at very high frequencies by performing an appropriate time scaling. This offers the possibility of using our coupled system for Ultra Wide Band (UWB) applications.

Keywords: Ultra Wideband Communication; Chaotic Modulation and Demodulation; UWB Positioning Systems.

1. Introduction

The last years have witnessed intensive studies of UWB communication systems. The interest devoted to such systems is motivated by the various potential advantages the UWB technology can bring to the wireless industry. Indeed, the UWB technology can solve the RF spectrum availability problem, improve the security, can provide less expensive, less power consuming equipment for a variety of wireless applications [1].

The basic idea of synchronization was to adjust the frequencies of weakly interacting periodic oscillators [2-5]. Nowadays several types of synchronization representing different degrees of correlation between the coupled systems have been identified: a) complete (or full) synchronization, b) generalized synchronization and, c) phase synchronization.

Full synchronization is achieved when the states of coupled systems coincide, while the dynamics in time remains chaotic. Generalized synchronization, as introduced for drive-response systems, is defined as the presence of some functional relationship between the states of the response and the drive. Phase synchronization is achieved when the phases of coupled systems lock to each other, while their amplitudes remain uncorrelated and sustain an irregular motion of their own [6]. To date, synchronization of chaos [7-9] has aroused much interest in light of its potential applications. In particular, the use of chaotic synchronization in communication systems has been investigated intensively [10-16]. The principle consists of the transmission of an information signal containing a message, using chaotic signal as a broadband carrier. The synchronization process is achieved to recover the information at the receiver. Due to the broadband feature of the chaotic signal, it can be used in UWB and communications systems in chaotic pulse position modulation [17].

We present in this report some effects of synchronization of coupled self-sustained non-identical chaotic Rössler oscillators. To characterize these phenomena, we use both numerical and analog simulation techniques. The experimental observation of chaotic oscillations in coupled nonlinear circuits is used to discuss some unknown forms of cooperative behaviour that are related to the regimes of synchronized chaos. One of the most important contributions of this work is to list some important and new problems encountered when synchronizing non-identical chaotic Rössler oscillators. Such a synchronization process can be achieved through the use of an auxiliary system (a third oscillator of the Rössler type), which is considered as the ideal predictor that is able to indicate the current state of the response system by processing the driving signal. A similar approach was carried out by Rulkov [18]. He considered simplified cases of non-identical synchronized chaotic oscillations that were observed in directionally coupled circuits with different parameter values and generalized the definition of chaos synchronization as the ability to predict the current state of the response system from the chaotic data measured from the driving system.

The general goal of this work is to adapt the study carried out by Rulkov [18] to the case of UWB Rössler generators: we use a class of synchronizing systems, which is unidirectional coupled non-identical Rössler systems (master-slave or drive-response configurations). The interest devoted to the Rössler system is motivated by their capability to behave chaotically at very high frequencies. Chaotically modulated oscillations and chaotic pulses are obtained and are shown as characteristic features of the oscillators. These oscillators are of great interest in UWB applications and communications [10, 19]. A technique of synchronization in case of chaotic modulation is presented. Numerical solutions

are compared with the experimental results and a very good agreement is obtained between the both methods. One of the interests of this work is to prove that analog computation is suitable than its numerical counterpart for understanding the real physical behaviour of chaotic systems. The complete system (drive (x_1, y_1, z_1) + response (x_2, y_2, z_2) + auxiliary (x_3, y_3, z_3)) is modelled by the following set of equations:

$$\dot{x}_{1,2,3} = -\omega_{1,2,3}y_{1,2,3} - z_{1,2,3} + \varepsilon_{1,2,3}(x_{2,1,1} + x_{3,3,2} - x_{1,2,3}) \quad (1.a)$$

$$\dot{y}_{1,2,3} = \omega_{1,2,3}x_{1,2,3} + a_{1,2,3}y_{1,2,3} \quad (1.b)$$

$$\dot{z}_{1,2,3} = f_{1,2,3} + z_{1,2,3}(x_{1,2,3} - U_{1,2,3}) \quad (1.c)$$

Where ω_i are the natural frequencies of the oscillators, ε_i are the coupling coefficients and a_i , f_i and U_i are the system parameters. The dots stand for time derivatives.

The paper is organized as follows. Section II presents the numerical study of the complete system. We present some results showing both phase synchronization (PS) and lag synchronization (LS). Section III is devoted to the analog simulation of the complete system. We present the electronic circuit of our simulator with the associated definitions of the parameters of the system model as functions of the circuit components. The section ends by comparing the results from the simulator with those of the direct numerical integration of the system model. In Section IV we deal with conclusions and proposals for further works.

2. Numerical Study

We use the fourth-order Runge–Kutta algorithm for the numerical analysis. For the sets of parameters used in this work, the appropriate step size is fixed to $\Delta t = 0.0005$ and the calculations are performed using real variables and constants in extended mode. The integration time is always greater than $T = 10^6$. Let us note that by changing the values of the system parameters, one should always control the step size used in order to prevent abrupt discontinuities that can automatically induce errors in computation.

2.1. Lag Synchronization

This subsection shows the achievement of lag synchronization when monitoring the coupling parameter ε_2 . For the following set of system parameters, $\omega_1 = 1.02$, $a_1 = 0.1125$, $f_1 = 0.38$, $U_1 = 11.49$, $\varepsilon_1 = 0.44$, $\omega_2 = 0.98$, $a_2 = 0.1230$, $f_2 = 0.20$, $U_2 = 10.9$, $\omega_3 = \omega_2$, $a_3 = a_2$, $f_3 = f_2$, and $U_3 = U_2$, the regime of LS is clearly demonstrated in Fig. 1 by plotting $x_2(t + \tau_0)$ versus $x_1(t)$. t is the time variable and τ_0 is the time shift or time lag. Fig. 1 shows the projection of the attractors of the drive and response systems onto the plane $(x_1(t), x_2(t))$ and delayed coordinates plots $x_2(t + \tau_0)$ versus $x_1(t)$. It is clearly shown that the transition for a non-synchronized state ($\varepsilon_2 = 0.10$) to a synchronized state ($\varepsilon_2 = 0.36$) is

achieved by increasing the coupling coefficient ε_2 . Mention that lag synchronization is achieved for the lag time $\tau_0 = 0.098$. Let us also mention that the achievement of lag synchronization in our model corresponds to the following equalities: a)- $x_2(t + \tau_0) \approx x_1(t) = x_3(t)$; b)- $y_2(t + \tau_0) \approx y_1(t) = y_3(t)$; c)- $z_2(t + \tau_0) \approx z_1(t) = z_3(t)$. Let us finally mention that the synchronization of pulse waves (coordinates z_i) was obtained with an almost constant small divergence (about 6%). Furthermore we found that the divergence observed were an increasing function of the integration step size. This help to underline the fact that the numerical study of Rössler systems needs the choice of very small integration step size.

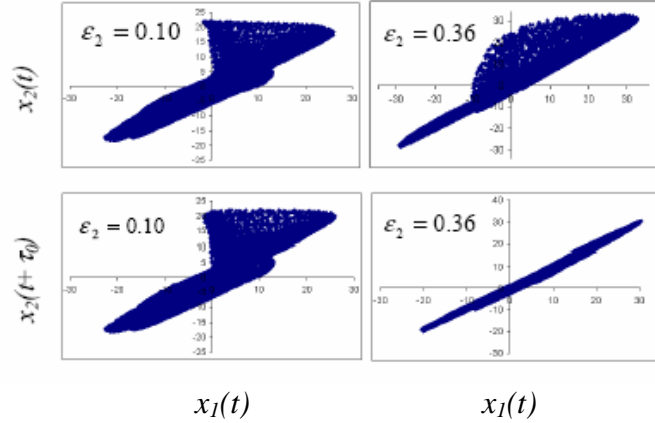


Figure 1. Projection of the attractors onto the planes $(x_1(t), x_2(t))$ and $(x_1(t), x_2(t + \tau_0))$ with $\tau_0 = 0.098$.

2.2. Phase Synchronization

The idea of phase synchronization of chaotic systems is close to synchronization of periodic oscillations. Here, only the phases are considered with no restriction on the amplitudes. Phase synchronization is achieved in our model when the phase difference between neighbouring oscillators does not grow with time but remains bounded. This condition can be materialized by the inequality $|\phi_2 - \phi_1| < Const$. ϕ_1 and ϕ_2 represent respectively the phases of both drive and response systems.

In the polar coordinates, Eqs. (1) can be written in the form

$$\begin{aligned} \frac{dr_{1,2,3}}{dt} = & r_{1,2,3} a_{1,2,2} \sin^2 \phi_{1,2,3} \\ & + [\varepsilon_{1,2,2} (r_{2,1,1} \cos \phi_{2,1,1} + r_{3,3,2} \cos \phi_{3,3,2} - r_{1,2,3} \cos \phi_{1,2,3}) - z_{1,2,3}] \cos \phi_{1,2,3} \end{aligned} \quad (2.a)$$

$$\begin{aligned} \frac{d\phi_{1,2,3}}{dt} = & \omega_{1,2,2} + a_{1,2,2} \cos \phi_{1,2,3} \sin \phi_{1,2,3} \\ & - \frac{\sin \phi_{1,2,3}}{r_{1,2,3}} [(r_{2,1,2} \cos \phi_{2,1,2} + r_{3,3,1} \cos \phi_{3,3,1} - r_{1,2,3} \cos \phi_{1,2,3}) \varepsilon_{1,2,2} - z_{1,2,3}] \end{aligned} \quad (2.b)$$

$$\frac{dz_{1,2,3}}{dt} = f_{1,2,2} + z_{1,2,3} (r_{1,2,3} \cos \phi_{1,2,3} - U_{1,2,2}), \quad (2.c)$$

taking into account the following definitions: $x_{1,2,3} = r_{1,2,3} \cos \phi_{1,2,3}$, and $y_{1,2,3} = r_{1,2,3} \sin \phi_{1,2,3}$.

Eqs. (2) are solved numerically using the Runge-Kutta algorithm. Considering the same sets of the system parameters in Fig. 1, we have analyzed the effect of the coupling ε_2 on the phase synchronization. Fig. 2 shows the variation of the phase difference between ϕ_1 and ϕ_2 in the time domain. We have found that for $\varepsilon_2 = 0.257$ the phase synchronization is not achieved and that by decreasing ε_2 leads to the phase synchronization (e.g. $\varepsilon_2 = 0.24$).

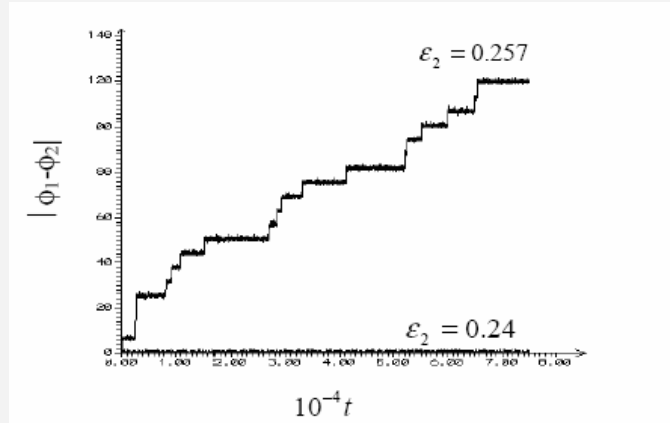


Figure 2. Phase difference of three coupled Rössler oscillators versus time with $\varepsilon_2 = 0.257$ (non-synchronized) and $\varepsilon_2 = 0.24$ (synchronized).

3. Experimental Study

The experimental study of the chaotic synchronization carried out in this work aims to verify the results obtained numerically. This study also aims to show that the analog simulator is a very powerful tool for the investigation of complex nonlinear models.

Fig. 3 is a scheme of the complete electronic simulator for the investigation of the dynamics of the drive-response-auxiliary system. In terms of the circuit components, the

parameters of the system model are defined as follows:

$$\omega_1 = \frac{10^{-4}}{R_{12}C_{11}}; \quad a_1 = \frac{10^{-4}R_{10}}{R_{13}R_{18}C_{12}};$$

$$f_1 = \frac{10^{-4}V_{cc}}{R_{15}C_{13}}; \quad U_1 = \frac{10^{-4}}{R_{16}C_{13}}; \quad \varepsilon_1 = \frac{10^{-4}}{R_{19}C_{11}}; \quad R_{11}C_{11} = 10^{-4}; \quad R_{14}C_{13} = 10^{-5}; \quad R_{10} = \frac{R_{13}R_{17}C_{12}}{R_{12}C_{11}};$$

$$\omega_2 = \frac{10^{-4}}{R_{22}C_{21}}; \quad a_2 = \frac{10^{-4}R_{20}}{R_{23}R_{28}C_{22}}; \quad f_2 = \frac{10^{-4}V_{cc}}{R_{25}C_{23}}; \quad U_2 = \frac{10^{-4}}{R_{26}C_{23}}; \quad \varepsilon_2 = \frac{10^{-4}}{R_{29}C_{21}}; \quad R_{21}C_{21} = 10^{-4};$$

$$R_{24}C_{23} = 10^{-5}; \quad R_{20} = \frac{R_{23}R_{27}C_{22}}{R_{22}C_{21}}; \quad \omega_3 = \frac{10^{-4}}{R_{32}C_{31}}; \quad a_3 = \frac{10^{-4}R_{30}}{R_{33}R_{38}C_{32}}; \quad f_3 = \frac{10^{-4}V_{cc}}{R_{35}C_{33}};$$

$U_3 = \frac{10^{-4}}{R_{36}C_{33}}$; $\varepsilon_3 = \frac{10^{-4}}{R_{39}C_{31}}$; $R_{31}C_{31} = 10^{-4}$; $R_{34}C_{33} = 10^{-5}$; $R_{30} = \frac{R_{33}R_{37}C_{32}}{R_{32}C_{31}}$. The time unit is $10^{-4} S$.

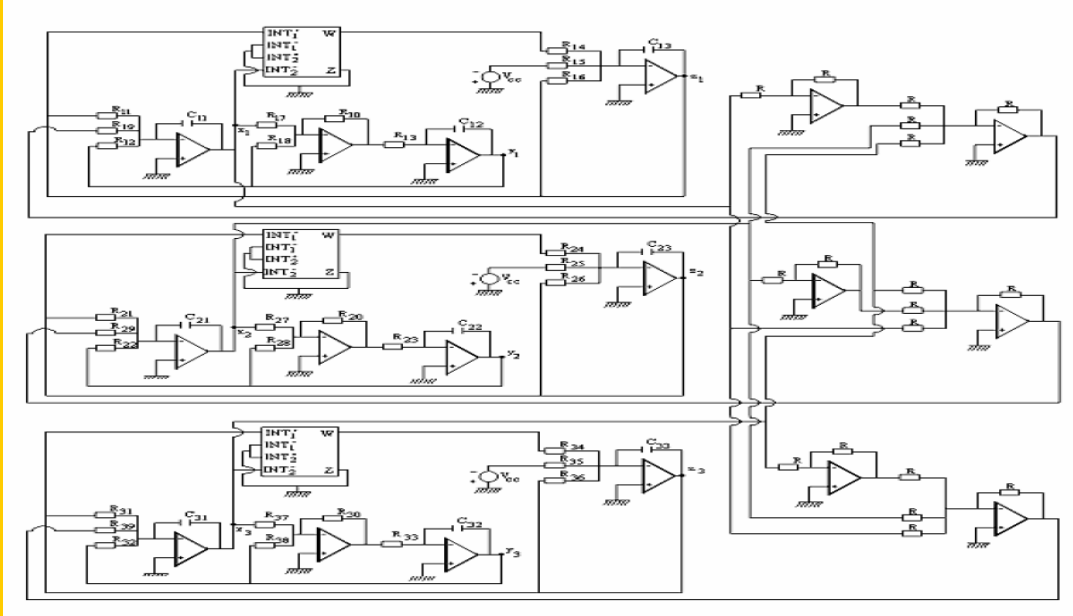


Figure 3. Scheme of the complete electronic simulator

In order to control each parameter of the system model by varying only one resistor, we set the following values of the circuit components: $V_{cc} = 1.15V$; $C_{11} = 9.73nF$; $C_{12} = 9.83nF$; $C_{13} = 10.67nF$; $C_{21} = 10.73nF$; $C_{22} = 10.25nF$; $C_{23} = 10.13nF$; $C_{31} = 10.73nF$; $C_{32} = 10.36nF$; $C_{33} = 10.16nF$; $R_{11} = 10800\Omega$; $R_{21} = R_{31} = 9320\Omega$; $R_{23} = R_{33} = 9950\Omega$; $R_{13} = 9960\Omega$; $R_{14} = 937\Omega$; $R_{24} = 987\Omega$; $R_{34} = 984\Omega$; $R_{15} = 9200\Omega$; $R_{25} = R_{35} = 10200\Omega$; $R_{17} = 1735\Omega$; $R_{27} = R_{37} = 1472\Omega$; $R_{10} = 2040\Omega$; $R_{20} = 2270\Omega$; $R_{30} = 1790\Omega$. Thus, the coefficients ε_1 , ε_2 , ω_1 , ω_2 , U_1 , U_2 , a_1 , a_2 , f_1 and f_2 will be controlled respectively by R_{19} , R_{29} , R_{12} , R_{22} , R_{16} , R_{26} , R_{18} , R_{28} , R_{15} and R_{25} . Note that the analog voltages obtained from our simulator are directly equivalent to the dimensionless variables of the system model. We now analyze the chaotic synchronization of non-identical oscillators (drive-response) experimentally. The set of system parameters used in the numerical study cannot be considered for the experiment, the dynamics of the simulator being limited by the power supply ($V_0 = \pm 15V$). This justifies the choice of the following values of resistors: $R_{12} = 8560\Omega$; $R_{22} = R_{32} = 7900\Omega$; $R_{18} = 5890\Omega$; $R_{28} = 6470\Omega$; $R_{38} = 5050\Omega$; $R_{16} = 2170\Omega$; $R_{26} = R_{36} = 2300\Omega$; $R_{19} = 82000\Omega$; $R_{29} = R_{39} = 99100\Omega$. These values correspond to a state where the chaotic waveforms from the drive and response systems are synchronized. Figs. 4a and 4b show respectively the experimental chaotic phase portrait of the auxiliary system and its corresponding numerical phase portrait in the decoupled state of the system. In Figs. 5a and 5b are shown respectively the experimental projection of the attractors of the systems (drive and response) onto the plane $(x_1(t), x_2(t))$ and its corresponding numerical one when the LS is achieved. The numerical values used to

achieve the synchronization are: $\omega_1 = 1.2$; $a_1 = 0.354$; $f_1 = 1.1659$; $U_1 = 4.3117$; $\varepsilon_1 = 0.125$; $\omega_2 = 1.18$; $a_2 = 0.344$; $f_2 = 1.1123$; $U_2 = 4.2796$; $\varepsilon_2 = 0.094$; $\omega_3 = 0.922$; $a_3 = a_2$; $f_3 = f_2$; $U_3 = U_2$; $\varepsilon_3 = \varepsilon_2$. Fig. 6 shows the corresponding chaotic experimental synchronized waveforms respectively in the drive (upper picture) and the response (lower picture) systems. The results obtained from our electronic simulator were generally very close to those obtained numerically. This helps to validate the results obtained in this work. One should note that LS is achieved numerically (case of Fig. 5) for a given detuning $\sigma = 0.258$ between the natural frequencies of both the auxiliary and response systems.

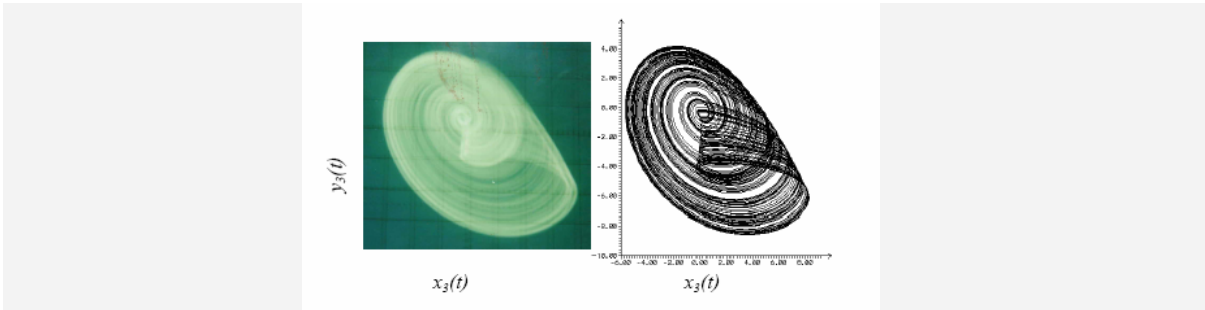


Figure 4. Chaotic phase portraits of the auxiliary system with the following values of the resistors: $R_{32} = 9600\Omega$; $R_{36} = 2300\Omega$; $R_{33} = 8340\Omega$; $R_{35} = 10100\Omega$. This corresponds to the following numerical values: $f_3 = 1.223$; $U_3 = 4.2796$; $\omega_3 = 0.97$; $a_3 = 0.41$ (the other values used in the case of chaotic synchronization remain unchanged).



Figure 5. Projection of the attractors onto the plane $(x_1(t), x_2(t))$ in the case of chaotic synchronization

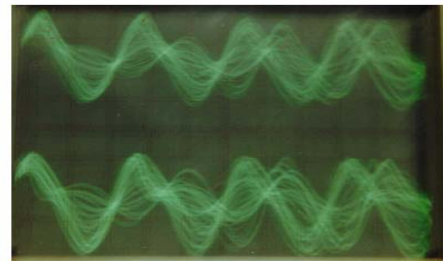


Figure 6. Pictures of the experimental synchronized chaotic waveforms in the drive (upper picture) and response (lower picture) systems

4. Conclusion

This paper has dealt with the study of a generalized case of synchronized chaos in drive-response systems. A predicting device (the auxiliary system) has been used as a replica of the response system. This auxiliary system was chosen to be driven in the same way as the response system (that is the parameters of the models describing both response and auxiliary systems are identical). We have shown the achievement of both LS and PS of chaotic oscillations in the drive-response systems when monitoring the coupling coefficient ε_2 . The experimental study of chaos synchronization was carried out using analog computer implementation techniques. The results from our electronic circuit were compared with the numerical results and we found a very good agreement between the two methods. This

perfect agreement has confirmed the fact that analog simulation is suitable than its numerical counterpart for the analysis of complex nonlinear systems. A very important problem under investigation is the experimental control of the lag time (τ_0) to achieve the experimental LS of chaotic oscillations.

Acknowledgements

The authors are very grateful for the financial supports received from both the Deutscher Akademischer Austausch Dienst (**DAAD**) (grant: A/03/15524, Desk: 413) and the Swedish International Development Cooperation Agency (**SIDA**) through the International Centre for Theoretical Physics (**ICTP**) Trieste, Italy. The authors are also grateful to Prof. Samuel Domngang (University of Yaoundé-I, Cameroon) for his helpful and constructive comments and recommendation on this work.

References

1. A. Volkovskii, I. Langmore, AIP Conference Proceedings, Vol.676, August, 2003.
2. A. Andronov, A. Vitt and S. Khykin, Theory of Oscillations, Pergamon Press, Oxford, 1966.
3. C. Hayashi, Nonlinear Oscillations in Physical Systems, McGraw-Hill, New York, 1964.
4. I. Blekhman, Synchronization of Dynamical Systems, Nauka, Moscow, 1971.
5. Arkady S. Pikovsky, Michael G. Rosenblum, Grigory V. Osipov, Jürgen Kurths, Physica D. Vol. 104, pp.219-238, 1997.
6. O. V. Sosnovtseva, A. G. Balanov, T. E. Vadivasora, V. V. Astakhov, E. Mosekilde, Phys. Rev. E, Vol.60, pp.6560-6565, 1999.
7. L. Pecora, and T. L. Carroll, Phys. Rev. Lett., Vol.64, pp.821-823, 1990.
8. T. L. Carroll, and L. Pecora, IEEE Trans. Circuits Syst. Vol.38, pp.453-456, 1991.
9. I. Blekhman, Synchronization in Science and Technology, ASME Press, New York, 1998.
10. K. M. Cuomo and A. V. Oppenheim, Phys. Rev. Lett, Vol.71, pp.65-68, 1993.
11. L. Kocarev, K. S. Halle, K. Eckert, L. O. Chua, U. Parlitz, Int. J. Bifurcation Chaos, Vol. 2, pp. 709-713, 1992.
12. R. Lozi, and L. O. Chua, Int. J. Bifurcation Chaos, Vol.3, pp.1319-1325, 1993.
13. K. M. Cuomo, A. V. Oppenheim and S. H. Strogatz, Int. J. Bifurcation Chaos, Vol.3, pp.1629-1638, 1993.
14. U. Parlitz, L. O. Chua, L. Kocarev, K. S. Halle and A. Shang, Int. J. Bifurcation Chaos, Vol. 2, pp. 973-977, 1992.
15. K. S. Halle, C. W. Wu, M. Itoh and L. O. Chua, Int. J. Bifurcation Chaos, Vol.3, pp.1619-1627, 1993.

16. C. W. Wu and L. O. Chua, *Int. J. Bifurcation Chaos*, Vol.3, pp.1619-1627, 1993.
17. M. Sushchik, N. Rulkov, L. Larson, L. Tsimring, H. Abarbanel, K. Yao, and A. Volkovskii, *IEEE Communication Lett.* Vol. 4, pp. 128-130, 2000.
18. N. F. Rulkov, *Special Focus Issue of Chaos*, Vol. 6, pp.262-279, 1996.
19. L. Kocarev, and U. Parlitz, *Phys. Rev. Lett.*, Vol.74, pp.5028-5031, 1993.